Terahertz Real-Time Off-Axis Digital Holography with Zoom Function *

Lei Hou(侯磊)[1,2], Xiao-Wei Han(韩小卫)[1,3], Lei Yang(杨磊)[1], Wei Shi(施卫)[1,2]**

[1]*Department of Applied Physics, Xi'an University of Technology, Shaanxi 710048*
[2]*National Key Laboratory of Science and Technology on Applied Physical Chemistry, Shaanxi 710061*
[3]*Institute of Physical and Electrical Engineering, Weinan Normal University, Weinan 714000*

(Received 16 January 2017)

We present a terahertz (THz) real-time digital holographic system with zoom function worked at 0.17 THz. The magnification factor ranges from 1 to 2. In the imaging experiment, the resolution is 2 mm with the magnification factor of 1.2. A metal sheet with F-shaped hollow is used as a sample, and its THz holograms are reconstructed by our developed algorithm based on the angular spectrum theorem, and the qualities of the THz images under different conditions are compared.

PACS: 42.40.−i, 42.15.Eq, 42.30.Va DOI: 10.1088/0256-307X/34/5/054207

Based on the unique excellent properties of terahertz (THz) waves,[1−3] the THz imaging technique plays a significant role in the areas of nondestructive detection, biomedicine, security check, and so on.[4−7] THz digital holography is a combinative production of the THz imaging technique and the digital holography technique. Compared with the conventional imaging technique, this kind of interferometry is able to obtain both the amplitude and the phase information of THz waves transmitted or reflected from an object, simultaneously.[8−10] Moreover, it can improve the image quality and can enhance the resolution of imaging systems. In 1996, Wu *et al.*[11] first proposed pulsed THz digital holography, and the method gained extensive attention and was used in imaging of chemicals,[12] recording the movement of a water drop,[13] and so on. Because cw THz sources have the advantages of high emission power, compact size, and low price, cw THz digital holography has more promising applications. In 2011, Heimbeck *et al.*[14] reported a THz off-axis digital holography system worked in 0.66–0.76 THz, and investigated the angular spectrum theorem to reconstruct the THz holography image. Recently, the THz off-axis digital holography system was optimized by a high-frequency THz source and the image reconstruction algorithm was improved.[15,16] In 2015, a real-time THz digital holography system was reported using a 2.8 THz quantum cascade laser as a source, its resolution can be as small as 200 μm and the image capture speed achieved 5 frame/s.[17] In the present study, we fabricate a real-time off-axis holography system with zoom function, and develop an image reconstruction algorithm under the conditions of the detector array on or off the imaging plane.

Figure 1 is the schematic diagram of the THz off-axis digital holography system. A Gunn oscillator (Virginia Diodes Inc.) acts as the source, which generates the THz wave with the frequency of 0.17 THz and the power of 50 mW. It can be regarded as a monochromatic source, since its bandwidth is less than 0.01 THz. The THz wave is collimated by a high-density-polyethylene (HDPE) lens (lens 1) with the focal length of 50 mm, and is divided into the object beam and the reference beam with the same power by a high-resistance silicon beam splitter. The reference beam is reflected on a THz pyroelectric array camera (Pyrocam Ⅲ, Spiricon corporation) by two metal mirrors (mirrors 1 and 2), which are also rotated vertically against the beam, ensuring the real and virtual images have a deviation in the frequency coordinate. The object beam is focused on the pyroelectric array camera by three HDPE lenses (lenses 2, 3 and 4) with the focal length of 50 mm. The sample is put between the beam splitter and lens 2. By adjusting the position of lens 3, we can achieve a tunable beam expanding ratio. The sensing area of the pyroelectric array camera is $12.4 \times 12.4\,\mathrm{mm}^2$ and the pixel size is $0.1\,\mathrm{mm} \times 0.1\,\mathrm{mm}$. An average of 15 frames was used to improve the signal-to-noise ratio (SNR) and the image capture rate was 3 frame/s, thus it is a real-time imaging system. The angle between the object beam and the reference beam is for separating and extracting the real or virtual images in frequency domain of the hologram. If the pyroelectric array camera is located at the image plane, the information of the object beam on the image plan can be obtained by carrying out the inverse Fourier transform to the filtered spectrum of the hologram. If the pyroelectric array camera is operated at a certain distance away from the image plane, the angular spectrum theorem is used to restore the complex amplitude at image plane.

THz intensity of the digital hologram recorded by the pyroelectric array camera in the x–y coordinate can be written as

$$\begin{aligned} I(x,y) &= |R(x,y) + O(x,y)|^2 \\ &= |R(x,y)|^2 + |O(x,y)|^2 \\ &\quad + R^*(x,y)O(x,y) \\ &\quad + R(x,y)O^*(x,y), \end{aligned} \tag{1}$$

*Supported by the National Natural Science Foundation of China under Grant Nos 61575161 and 61427814, the Foundation of Shaanxi Key Science and Technology Innovation Team under Grant No 2014KTC-13, the Special Financial Grant from the China Postdoctoral Science Foundation under Grant No 2013T60883, and the Equipment Pre-research Fund Project of China under Grant No 9140C370504140C37175.

**Corresponding author. Email: swshi@mail.xaut.edu.cn

where I represents the THz intensity, R and O are the complex amplitudes of the reference beam and the object beam, R^* and O^* are their conjugate variables, respectively. In the process of reconstructing object wavefront from the hologram, real and virtual images always appear together with a dc term generated by zero-order diffraction light in frequency domain. Because the THz wave has a spatial frequency bandwidth, the dc term, real and virtual terms can be separated in this domain by forming an appropriate angle between the object beam and the reference beam. When the angle exceeds $\sin^{-1}(3\lambda B)$, those three terms can be distinctly isolated, where λ and B are the wavelength and the bandwidth of THz wave, respectively. Figure 2 illustrates the distribution of the reference beam, the object beam, the object beam and the conjugated object beam and their separation condition in the spectrum, and u_1, u_2, u_3 and u_4 represent the reference beam intensity, the object beam intensity, the object beam amplitude and the conjugated object beam amplitude, respectively.

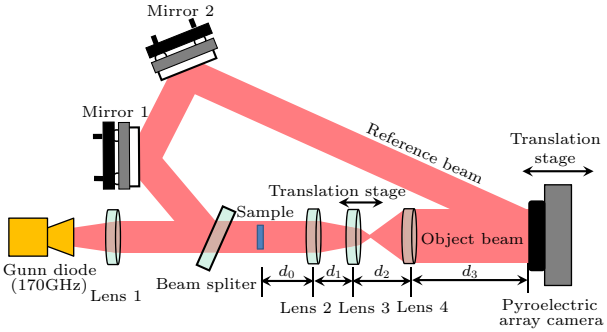

Fig. 1. Schematic diagram of the THz off-axis digital holography system.

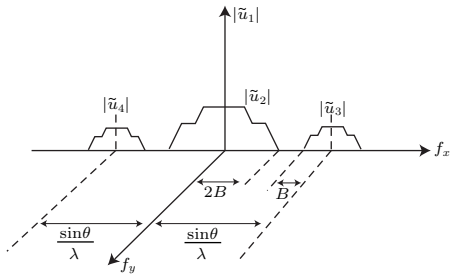

Fig. 2. Distribution of reference beam, object beam, object beam and conjugated object beam and their separation condition in the spectrum.

Because the wavelength of the THz source is large, the angle between these two beams will easily satisfy the requirement of the Nyquist sampling theorem, even if it approaches the right angle. In this experiment, the angle is 40° due to the restriction of optical elements' size. When the pyroelectric array camera is not placed at image plane rightly, we can use the angular spectrum theorem to reconstruct the object light wavefront after the real or virtual image is achieved by windowed filtering in frequency domain. This method is more precise than the commonly used Fresnel holographic reconstruction method.[18]

The process of the propagation pattern can be expressed as

$$U(x,y,z) = F^{-1}(F\{U(x,y,0)\} \cdot \exp\left[j\frac{2\pi}{\lambda}z\sqrt{1-(\lambda f_x)^2-(\lambda f_y)^2}\right]), \quad (2)$$

where $U(x,y,0)$ represents the complex amplitude on diffraction screen, $U(x,y,z)$ represents that on the receiving screen, f_x and f_y are spatial frequencies on the diffraction screen, and z is the distance between these two screens.

Based on the matrix optics theorem, the optical transformation matrix between lenses 2 and 4 can be written as

$$M_1 = \begin{bmatrix} A_1 & B_1 \\ C_1 & D_1 \end{bmatrix}, \quad (3)$$

$$A_1 = 1 - \frac{d_1+2d_2}{f} + \frac{d_1 d_2}{f^2}, \quad (4)$$

$$B_1 = d_0 + d_1 + d_2 - \frac{d_0 d_1 + 2d_0 d_2 + d_1 d_2}{f}, \quad (5)$$

$$C_1 = -\frac{2f - d_1}{f^2}, \quad (6)$$

$$D_1 = 1 - \frac{2d_0 + d_1}{f} + \frac{d_0 d_1}{f^2}, \quad (7)$$

where f is the focal length of the lens, d_0, d_1 and d_2 represent the distance between sample and lens 2, the distance between lenses 2 and 3, and the distance between lenses 3 and 4, respectively. According to Eq. (6), the combined focal length of lenses 2 and 3 ranges from $f/2$ to f. Correspondingly, the magnification ranges from 1 to 2. To ensure the exact image plane, the optical transformation matrix of the system is expressed as

$$\begin{aligned} M_2 &= \begin{bmatrix} 1 & d_3 \\ 0 & 1 \end{bmatrix}\begin{bmatrix} 1 & 0 \\ -\frac{1}{f} & 1 \end{bmatrix}\begin{bmatrix} 1 & d_2 \\ 0 & 1 \end{bmatrix}\begin{bmatrix} 1 & 0 \\ -\frac{1}{f} & 1 \end{bmatrix} \\ &\cdot \begin{bmatrix} 1 & d_1 \\ 0 & 1 \end{bmatrix}\begin{bmatrix} 1 & 0 \\ -\frac{1}{f} & 1 \end{bmatrix}\begin{bmatrix} 1 & d_0 \\ 0 & 1 \end{bmatrix} \\ &= \begin{bmatrix} A_2 & B_2 \\ C_2 & D_2 \end{bmatrix}, \end{aligned} \quad (8)$$

$$A_2 = 1 + d_1 d_2 + d_1 d_3 - \frac{d_1 + 2d_2 + 3d_3 - d_1 d_2 d_3}{f} + \frac{d_1 d_3 + 2d_2 d_3}{f^2}, \quad (9)$$

$$\begin{aligned} B_2 = {} & d_0 + d_1 + d_2 + d_3 \\ & - [d_0 d_1 + 2d_0 d_2 + 3d_0 d_3 + 2d_1 d_3 \\ & + d_1 d_2 + d_2 d_3]/f \\ & + \frac{2d_0 d_1 d_3 + d_0 d_1 d_2 + 2d_0 d_2 d_3 + d_1 d_2 d_3}{f^2} \\ & - \frac{d_0 d_1 d_2 d_3}{f^3}, \end{aligned} \quad (10)$$

$$C_2 = d_1 - \frac{d_1 d_2 + 3}{f} + \frac{d_1 + 2d_2}{f^2}, \tag{11}$$

$$D_2 = 1 - \frac{3d_0 + 2d_1 + d_2}{f} + \frac{2d_0 d_1 + 2d_0 d_2 + d_1 d_2}{f^2} - \frac{d_0 d_1 d_2}{f^3}, \tag{12}$$

where d_3 represents the distance between lens 4 and the pyroelectric array camera, and A_2 describes the lateral magnification of the system. The Fresnel number is expressed by

$$F = \frac{a^2}{\lambda}\left(\frac{A_2}{B_2} + \frac{1}{R^2}\right),$$

where a is the diffraction aperture, and R means the curvature radius of spherical wave. According to the geometrical optics theory, the diffraction effect can be ignored when the Fresnel number tends to infinity and THz wave exactly right locates the image plane. In our experiment, the incident THz wave on the sample is a parallel wave, which means that R approaches zero. Therefore, the image plane can be identified when item B_2 is equal to zero. Therefore, the complex amplitude of the object light can be restored without complicated diffraction calculation, when the pyroelectric array camera is just placed at the image plane.

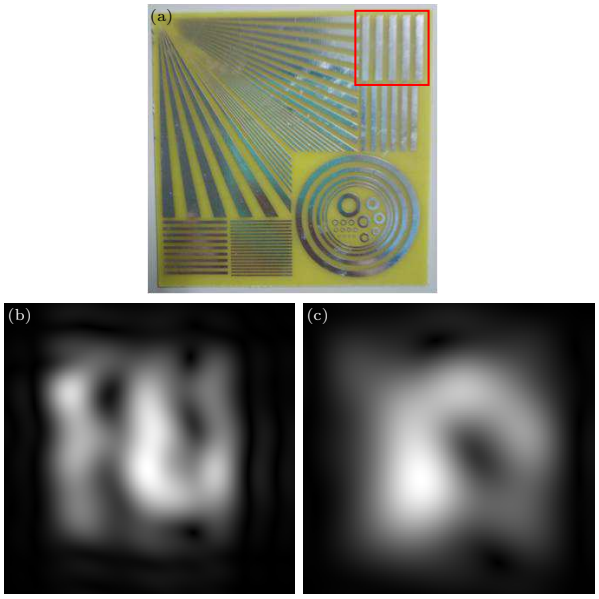

Fig. 3. (a) Photo of a resolution testing card. (b) THz image of metal pattern on the right up corner of the card when the magnification factor is 1.2. (c) THz image of the same area when the magnification factor is 1.

To evaluate the resolution of the off-axis digital holography system, the theoretical value was calculated by the Rayleigh criterion, and experimentally testified by a resolution testing card.

According to the Rayleigh criterion

$$d = \frac{0.61\lambda}{NA}, \tag{13}$$

where NA is the numerical aperture of objective lens. When the magnification factors are 1.2 and 1, the calculated limiting resolutions are 2.1 mm and 2.4 mm, respectively. Figure 3(a) is the photo of the resolution testing card, which is a teflon sheet covered by different metal patterns. The pattern on the right-upper corner of resolution testing card is a series of metal strip with the width of 2 mm and the gap of 2 mm, and it was used to measure the resolution of the system. Figures 3(b) and 3(c) are the measured results when the magnification factors are 1.2 and 1. In Fig. 3(b), three bright fringes can be recognized, which means that the resolution of the system can reach 2 mm. However, the metal patterns cannot be distinguished in Fig. 3(c). Thus the resolution can be improved by adding zoom function in the THz off-axis digital holography system.

In the THz holographic imaging experiment, a metal film with F-shaped hollow was used as a sample, and its photo is shown in Fig. 4(a). The width and length of F-shaped area are about 8 mm and 10 mm and the width of hollow area is roughly 2 mm. To make the image of the sample fill the window of the pyroelectric array camera, the distance between lenses 2 and 3 was set as 40 mm, and the magnification was 1.2. The sample was placed at 48 mm ahead of lens 2 and the pyroelectric array camera was placed at 80 mm behind lens 4. The angle between object beam and reference beam was 40°. Mirrors 1 and 2 have a certain pitch for taking advantage of spatial spectrum. Figure 4 is the directly detected holographic image of the sample. It is very difficult to identify the character of F. Then, the image reconstruction algorithm was used to obtain the image of the sample.

When the pyroelectric array camera was placed at the image plane, we calculate the spectrum of hologram by using fast Fourier transform (FFT) and reconstruct the object light wavefront. The positions of the object light center and the conjugate object light center in spatial spectrum can be calculated by

$$\frac{\sin\theta}{\lambda} \cdot \Delta x \cdot N, \tag{14}$$

where θ is the angle between the object beam and the reference beam, Δx is the pixel size, and N is the number in the FFT transform. By assigning a rectangular window with appropriate size, the real image or virtual image can be extracted. Then an inverse fast Fourier transform operation was used to restore the complex amplitude. The reconstructed image is shown in Fig. 4(c). The profile of F in the reconstructed image is clear. However, because the object beam partially overlapped with zero-order diffraction beam and the size of filter window was limited, partially high frequency information of the wavefront of reconstructed object beam or its conjugate beam was lost, which causes the distortion at some regions.

When the pyroelectric array camera located off the image plane, the angular spectrum theorem was used to inverted object light wavefront. However, this inverse diffraction operation might cause more losses of high frequency information, which will make the image fuzzier. Figures 4(d) and 4(e) show the results after employing the angular spectrum theorem when the pyroelectric array camera locates at 5 mm and 10 mm

away from the image plane. According to Eqs. (9)–(11), the Fresnel number is affected by d_3. Increasing d_3 causes more obvious diffraction, thus more high frequency information will be lost during the image reconstruction. We can still identify the character of F in Fig. 4(d), but the reconstructed image becomes so fuzzy that the F cannot be recognized in Fig. 4(e).

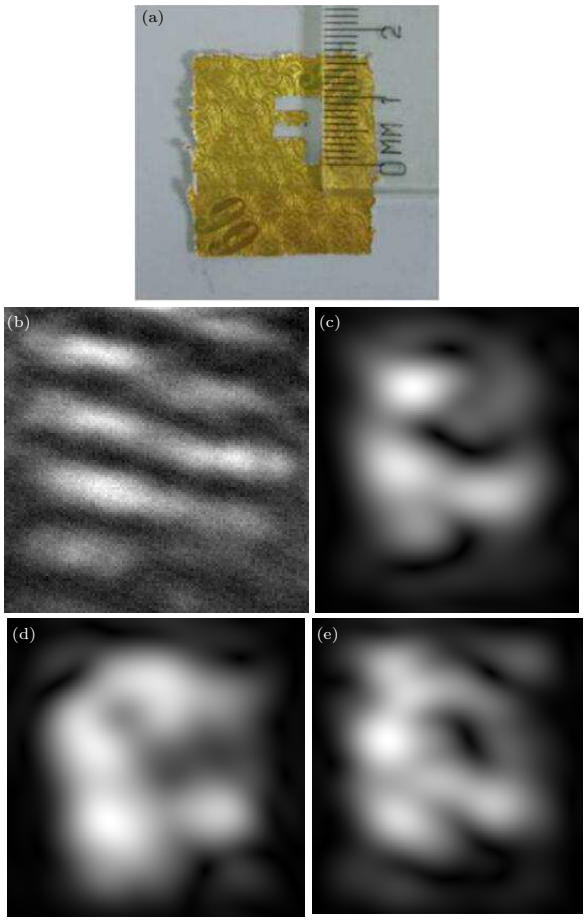

Fig. 4. (a) Photo of the sample. (b) Directly detected holographic image of the sample. (c) Restored THz image when the pyroelectric array camera is placed at image plane. (d) Restored THz image when the pyroelectric array camera is placed 5 mm far away from image plane. (e) Restored THz image when the pyroelectric array camera is placed 10 mm far away from image plane.

In summary, we have developed a terahertz real-time off-axis digital holography system with zoom function. It uses a 0.17 THz Gunn diode as the THz source and a pyroelectric array camera as detector array. The magnification factor of the system ranges from 1 to 2. In the imaging experiment, the magnification factor is set as 1.2 and the resolution is 2 mm. The THz images of a sample are obtained by carrying out the inverse fast Fourier transform to the filtered spectrum of the hologram when the pyroelectric array camera is on the image plane. Angular spectrum theorem is investigated to restore the complex amplitude of object wave, when the detector array is placed off the image plane. The results show that increasing the distance between pyroelectric detector array and the image plane will cause more obvious diffraction, and the restored image will become fuzzy since more high frequency information lost during the image reconstruction.

References

[1] Shen Y C, Lo T, Taday P F, Cole B E, Tribe W R and Kemp M C 2005 *Appl. Phys. Lett.* **86** 241116
[2] Exter M, Fattinger C and Grischkowsky D 1989 *Opt. Lett.* **14** 1128
[3] Tonouchi M 2007 *Nat. Photon.* **1** 97
[4] Hu B and Nuss M C 1995 *Opt. Lett.* **20** 1716
[5] Kawase K, Ogawa Y, Watanabe Y and Inoue H 2003 *Opt. Express* **11** 2549
[6] Mittleman D M, Gupta M, Neelamani R, Baraniuk R G, Rudd J V and Koch M 1999 *Appl. Phys.* B **68** 1085
[7] Chen H T, Kersting R and Cho G C 2003 *Appl. Phys. Lett.* **83** 3009
[8] Hariharan P 1996 *Optical Holography: Principles, Techniques and Applications* (Cambridge: Cambridge University Press)
[9] Smith H M 1977 *Basic Holographic Principles* (Berlin: Springer)
[10] Vest C M 1979 *Holographic Interferometry* (New York: John Wiley and Sons)
[11] Wu Q, Litz M and Zhang X C 1996 *Appl. Phys. Lett.* **68** 2924
[12] Usami M, Yamashita M, Fukushima, Otani K C and Kawase K 2005 *Appl. Phys. Lett.* **86** 141109
[13] Yasuda T, Kawada Y, Toyoda H and Takahashi H 2007 *Opt. Express* **15** 15583
[14] Heimbeck M S, Kim M K, Gregory D A and Everitt H O 2011 *Opt. Express* **19** 9192
[15] Bei S, Liu X, Ge X and Guo C 2014 *Opt. Express* **22** 23066
[16] Qi L, Ding S, Li Y, Xue K and Wang Q 2012 *J. Infrared Milli. Terahz. Waves* **33** 1039
[17] Massimiliano L, Ravaro M, Bartalini S, Consolino L, Vitiello M S, Cicchi R, Pavone F and Natale P D 2015 *Sci. Rep.* **5** 13566
[18] Kim M K, Yu L and Mann C J 2006 *J. Opt. A-Pure Appl. Opt.* **8** 518